

## Partial replacement of portland cement by bamboo ashes

Marcelly de Figueiredo Mendonça<sup>1</sup>, Marcelo Martins Farias<sup>1</sup>, Celestina Lima de Rezende Farias<sup>2</sup>,  
Marcelo de Souza Picanço<sup>1</sup>, Alcibiades Negrão Macêdo<sup>1</sup>

<sup>1</sup>Universidade Federal do Pará, Grupo de Análise de Estruturas e Materiais, Rua Augusto Corrêa, 01, Guamá, Belém, PA, Brasil.

<sup>2</sup>Instituto Federal de Educação, Ciência e Tecnologia do Pará, Laboratório de Edificações, Avenida dos Bragançanos, s/n, Vila Sinhá, Bragança, PA, Brasil.

e-mail: marcellyfmendonca@gmail.com, marcelofariasmmf@gmail.com, celestinarezende2006@gmail.com, marcelosp@ufpa.br, alcebiadesnm@ufpa.br

### ABSTRACT

Partial replacement of Portland cement by industrial waste or materials of natural origin can improve the mechanical strength of concrete and mortar and reduce production cost. In this context, ash from burning bamboo appears as a potential material for use, as it is natural with a renewable source and fast growth, which presents a higher concentration of silica in the outer walls of the stalks. Therefore, the objective of this work is to evaluate the use of bamboo stalk ash (*Bambusa Vulgaris*) as a partial replacement for Portland cement. For this purpose, bamboo ash was produced at three calcination temperatures (500°C, 600°C and 700°C). The ashes were not characterized as pozzolans based on their chemical composition, however the ash produced at 600°C obtained a performance index higher than that established by the Standard. The hydration of cement partially replaced by this ash was evaluated, in proportions of 0%, 6%, 10% and 14%, in relation to its mass. Mortars with the same replacement proportions were evaluated in the fresh state and hardened. The consistency in the fresh state remained constant at 227 mm, while the compressive strength, in the hardened state, increased by 15% with the addition of bamboo stem ash.

**Keywords:** Bamboo thatch ash; portland cement; partial replacement.

### 1. INTRODUCTION

More than fifty years ago, researchers already found that the world's most widely used building material is concrete. This is produced from a mixture of Portland cement, aggregates, and water. At that time, 63 million tons of cement were converted into 500 million tons of concrete per year, and its consumption, in mass, was already five times greater than that of steel. The success of this material is mainly due to its excellent water resistance, easy moldability in different shapes, relatively low cost, and availability in the market [1].

The search for the coexistence of technological development with environmental preservation is a significant challenge faced by the cement industry. Besides the high energy consumption and CO<sub>2</sub> emissions, there is the problem of exploitation of natural raw materials used, mainly limestone and clay. Moreover, the calcination of these raw materials in the manufacture of cement clinker is a significant carbon dioxide gas released into the atmosphere. According to Moir [2], a way to minimize all this is to partially replace clinker with industrial waste or materials of natural origin with a renewable source. Besides advantages for the environment, this possibility of replacement can improve specific properties of concrete and reduce its cost.

Bamboo is a vegetal material with the potential to use its ashes as a partial replacement for cement. It is a natural resource that renews itself in a shorter time interval [3], and Brazil has the most considerable diversity and highest index of endemic forests in Latin America [3]. However, in the country, its use is still quite early, and, except for the production of paper, it is destined for traditional applications, such as handicrafts, fishing rods, and furniture, among others [3].

Given the environmental problems generated in cement manufacture and the incipient destination of bamboo plantations in Brazil, this work aims to evaluate the potential use of bamboo thatch ash as a partial replacement for Portland cement. This proposal has several advantages, linked to the incorporation of mineral admixtures in Portland cement and the use of bamboo as a raw material.

Mineral admixtures are finely ground materials added to cement, usually of natural origin, and can be used in their original form or after treatment. Over time, various industrial wastes have become the primary sources of additions. The incorporation of mineral admixtures into the composition of Portland cement has many environmental, economic and technological benefits.

The main environmental benefit is the partial replacement of Portland clinker by the addition. The types of cement composed of mineral additions have lower costs since they replace a high-cost manufacturing material (clinker) with lower-cost ones. At the technological level, such additions also positively affect the technological performance of cement, such as increased mechanical strength and greater durability.

The use of bamboo as a raw material is justified once it is a natural material, with a renewable source and fast growth. Its cultivation does not require particular soil. In bamboo, silica is concentrated mainly in the outermost parts of the canes. Fast-growing plants tend to have a more significant amount of silica than slower-growing ones.

Silica stands out among the inorganic components of bamboo. After the calcination of the bamboo stalks, the organic matter is eliminated, resulting in ash-rich in silica. Siliceous materials, among other factors, have the potential to be used as a pozzolanic mineral admixture. The silica in the pozzolans reacts with the calcium hydroxide produced in the Portland cement hydration and produces more resistant materials, bringing technical benefits. Even though bamboo thatch ash does not present significant reactivity when incorporated into Portland cement, it can produce a physical effect due to the densification of the matrix by filling the pores of the mixture with fine inert material.

Incorporating bamboo stalks ash into Portland cement brings many benefits to the environment. First, it reduces the number of greenhouse gases and exploitation of raw materials generated in the manufacture of Portland clinker by incorporating a natural origin with a source of rapid renewal (bamboo). Second, it can positively affect the material's performance, such as greater mechanical strength. Finally, it would reduce the cost of the product.

Bamboo belongs to the subfamily Bambusoideae of the family Poaceae and is divided into three groups: Arundinarieae, Bambuseae, and Olyreae [4]. Most bamboo species thrive in temperatures between 8°C and 36°C and are naturally distributed across all continents except the European. Asia has the most native species, about 62%, followed by the Americas (34%), Africa (4%), and Oceania (4%) [5]. The worldwide geographical distribution of bamboos can be seen in Figure 1.

In Brazil, there are 258 species of bamboos distributed in two tribes, Bambuseae and Olyreae, and 35 genera, 12 genera and 175 species are endemic. The tribe Bambuseae has larger, lignified and woody stems and contains 18 genera and 165 species, while the tribe Olyreae has smaller herbaceous bamboos divided into 17 genera and 93 species [7, 10]. The most common species in the country are *Bambusa vulgaris vittata* (imperial bamboo), *Bambusa vulgaris* (green bamboo), *Bambusa tuldoides* (common bamboo), *Dendrocalamus giganteus*



**Figure 1:** Geographical distribution of bamboos in the world ([6] adapted).

(giant bamboo or bamboo-balde) and some species of the genus *Phyllostachys*. Being of Asian origin, these species were brought by the first immigrants and were disseminated throughout the country, due to their good adaptation to the Brazilian tropical climate [8].

Although Brazil is the country with the greatest diversity of woody bamboo species in the Americas, with 81% of the genera [7], its exploitation is still small compared to its versatility. Countries like Colombia and Ecuador use bamboo as a popular construction material and in agro-industries, enhancing rural development. Although the exploitation of bamboo in Brazil is subject to Law No. 12,484 of September 8, 2011 – which encourages its cultivation and sustainable management – there is still a lack of greater technological input for the production of stalks with standards for commercialization. The National Policy of Incentive to the Sustainable Management and Cultivation of Bamboo (PNMCB) recognizes a need for much investment in the production chain of bamboo so that it is valued as an efficient agro-silvo-cultural product that serves as a source of income for family farming [7].

Although bamboo is considered one of the main non-timber forest products, it is a suitable alternative to wood in activities that seek sustainable development since it can rapidly sequester atmospheric carbon, besides having excellent physical and mechanical characteristics [9]. According to MOGNON *et al.* [9], the most extensive carbon stock in bamboos is concentrated in the stems, followed by branches and leaves. This amount also varies according to the species.

The use of bamboo as a raw material has many advantages. The first one would be its fast growth since it takes much less time than any other tree to achieve its growth, about 4 to 5 years. It is also easy to plant, harvest, and maintain since there is no need to use pesticides and fertilizers when planting it, harvesting is done manually, and transportation is favored because it is lighter than wood. Another advantage is the versatility of bamboo, which has several applications, such as fuel, in paper manufacturing, civil construction, and the food and textile sectors. By replacing wood, bamboo also reduces the environmental impact caused by deforestation, besides contributing to the reduction of soil [10].

## 2. MATERIALS AND METHODS

This study was divided into four stages. First, it was the production of bamboo thatch ash (CCB) from calcination at three different temperatures. Secondly, the ashes' characterization to verify their mineralogical, physical, chemical, and pozzolanic properties were performed. Analysis was also made to determine the most suitable bamboo calcination temperature. The third step consisted of analyzing the hydration of the cement partially replaced by the bamboo thatch ash from the production of pastes. The fourth step consisted of producing mortars with the partial replacement of cement with bamboo ash. The mortars were evaluated in the fresh and hardened states. Table 1 describes the steps and methods applied in the experimental program.

**Table 1:** Experimental program.

| RESEARCH DESIGN                     | EQUIPMENT/METHOD      | MATERIAL/SAMPLES         |
|-------------------------------------|-----------------------|--------------------------|
| CCB production                      |                       |                          |
| Calcination (500°C, 600°C e 700°C)  | Electric Muffle       | Bamboo stem sawdust      |
| Grinding (1h, 2h, 4h, 6h e 8h)      | Ball Mill             | CCB500, CCB600 e CCB700  |
| Characterization of the CCB         |                       |                          |
| Particle size analysis              | Laser granulometry    | CCB500, CCB600 e CCB700  |
| Determination of the gravity weight | NBR 16605(ABNT, 2017) | CCB500, CCB600 e CCB700  |
| Mineralogical Analysis              | X-ray diffraction     | CCB500, CCB600 e CCB700  |
| Chemical Composition                | X-ray Fluorescence    | CCB600                   |
| Pozzolanicity                       | NBR 5752 (ABNT, 2014) | CCB500, CCB600 e CCB700  |
| Hydration evaluation in pastes      |                       |                          |
| Mineralogy of pastes                | X-ray diffraction     | PCB0, PCB6, PCB10 e PC14 |
| Thermogravimetry of the pastes      | TG/DTG Curves         | PCB0, PCB6, PCB10 e PC14 |
| Mortar behavior                     |                       |                          |
| Consistency (fresh state)           | NBR 7215 (ABNT, 1996) | ACB0, ACB6, ACB10 e AC14 |
| Compressive strength                | NBR 7215 (ABNT, 1996) | ACB0, ACB6, ACB10 e AC14 |
| Microstructure                      | SEM                   | ACB0, ACB6, ACB10 e AC14 |

## 2.1. MATERIALS

### 2.1.1. Portland cement

The performance index with Portland cement was determined at 28 days. The test used Portland cement composed of filler (called CP II-F) strength class 32 MPa, as prescribed by NBR 5752 [11]. A Brazilian high initial strength Portland cement (CP V-ARI) was also used in this study. CP V-ARI is the purest cement (higher amount of clinker) among those available in Brazil, enabling more accurate analysis regarding the behavior of bamboo stem ash used as a partial replacement for cement. The cement’s gravity weight was determined according to the NBR 16605 [12] (Table 2).

### 2.1.2. Fine aggregate

The fine aggregate used in the research was quartz sand from riverbeds near the metropolitan region of Belém. The aggregate underwent a previous drying process in an oven so that its humidity did not interfere with the water/cement ratio of the mortars. The characterization of the sand used is shown in Table 3, so that the gravity weight was determined according to NBR NM 52 [13], the unit mass and the voids index according to NBR NM 45 [14], and the fineness module according to NBR 7211 [15].

According to the particle size curve (Figure 2) obtained according to NBR 7211 [15], the sand used in the research fits in the inferior usable zone, being characterized as a very fine material.

### 2.1.3. Mixing water

To produce the cementitious matrices, tap water from the Cidade Universitária Professor José da Silveira Netto (UFPA’s campus in Belém) was supplied by its water treatment station.

### 2.1.4. Bamboo stalk ash (CCB)

The bamboo used for the production of ash belongs to the *Bambusa Vulgaris* species from the metropolitan region of Belém. The stems of this material were supplied by the Empresa Brasileira de Pesquisa Agropecuária – EMBRAPA – Amazônia Oriental and cut into approximately 1 meter long (Figure 3a) due to the easiness of

Table 2: Cement’s gravity weight.

| TYPE OF CEMENT | GRAVITY WEIGHT (g/cm <sup>3</sup> ) |
|----------------|-------------------------------------|
| CP II-F-32     | 3.08                                |
| CP V-ARI       | 2.99                                |

Table 3: Characteristics of the fine aggregate.

| GRAVITY WEIGHT         | UNIT MASS              | VOID INDEX | FINENESS MODULE |
|------------------------|------------------------|------------|-----------------|
| 2.57 g/cm <sup>3</sup> | 1.61 g/cm <sup>3</sup> | 37.35%     | 1.95            |

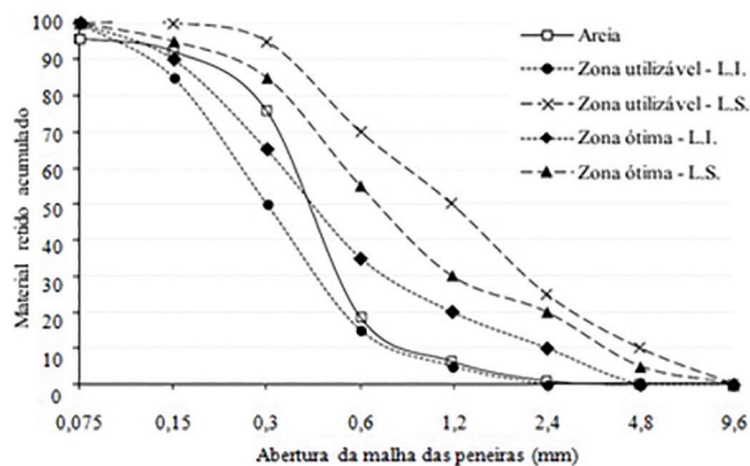


Figure 2: Sieve Size Curve of Sand and Limits of the Optimal and Usable Zones.

transportation. Before producing the ash, the stalks were cut into smaller pieces and later submitted to a knife and hammer mill (Extraction Center of the Chemistry College of UFPA). It was removed with a sawdust aspect (Figure 3b). Due to the grinding, the smaller the size of the grains, the greater the specific surface of the material, enabling an increase in chemical reactions and giving greater compactness to the mixture.

The ground bamboo was transformed into ash from the calcination process, carried out in a micro-processed muffle furnace (Figure 4) with 3720w of power and 220V (Materials Plant of the Chemical Engineering College of UFPA). Several authors have already characterized the ashes from bamboo leaves [24–28]. However, the characterization of ashes from bamboo stalks is still incipient; only the work developed by RODIER *et al.* [21] is a reference. The bamboo stalks from these cited researchs were calcined in three temperatures 500°C, 600°C and 700°C. To correlate the calcination temperature at which the bamboo thatch ash was produced and its respective physical and mineralogical characteristics. The ashes were named according to the temperature at which they were produced, as shown in Table 4.

The ground bamboo remained at a constant temperature for two hours. Four porcelain containers were used so that the material was deposited inside the muffle, avoiding contamination. The cooling was slow inside the muffle, which was opened 24 hours after it was turned off.



**Figure 3:** (a) Bamboo stalks; (b) Ground bamboo.



**Figure 4:** Muffle furnace used in the research.

**Table 4:** Nomenclature of bamboo stalk ash.

| NOMENCLATURE | CALCINATION TEMPERATURE |
|--------------|-------------------------|
| CCB500       | 500°C                   |
| CCB600       | 600°C                   |
| CCB700       | 700°C                   |

## 2.2. METHODS

### 2.2.1. Characterization of bamboo stalk ash

CCB500, CCB600 and CCB700 were submitted to mineralogical, physical, chemical and pozzolanic analyses. These analyses allowed determining the potential use of CCB in Portland cement matrices.

#### 2.2.1.1. Grinding

After the calcination process, the ashes of the bamboo thatch were submitted to grinding in a horizontal ball mill (Figure 5) in the Civil Engineering Laboratory of UFPA – LEMAC. The proportion of 5 kg of balls for 1 kg of ash was used, being 2/3 small balls and 1/3 large balls, according to the methodology used by POUEY [22]. The ashes were ground at 1, 2, 4, 6 and 8 hours and later submitted to laser granulometry analysis.

#### 2.2.1.2. Particle size analysis

The methodology of laser particle size analysis consisted of 1 g of material in 7 ml of distilled water, which was pipetted into a dispersion unit that also uses water as a suspension liquid. A laser particle analyzer model Analysette 22 Micro-Tec Plus from Fritsch GmbH, with a measuring range of 0.08 to 2000  $\mu\text{m}$ , was used to generate the particle size curves of the ash. This analysis was performed in the Laboratory of Mineralogy, Geochemistry and Applications of the Institute of Geosciences of UFPA.

#### 2.2.1.3. Determination of gravity weight

The determination of the gravity weight was performed at LEMAC, according to NBR 16605 [12]. The test was performed twice in each of the samples produced with different calcination temperatures.

#### 2.2.1.4. X-ray diffraction

The analysis was performed in the Research Laboratory of the Physics School of UFPA, in a BRUKER model D8 ADVANCE diffractometer. The High Score Plus software was used to identify minerals in the diffractogram peaks. The conditions for the analysis were: i) radiation: Cu K $\alpha$ ; ii) voltage: 40 kV; iii) current: 40 mA; iv) scanning with a 0.02° 2 $\theta$  step; v) time per step: 0.3s; vi) scanning interval: 5 to 60° (2 $\theta$ ); vii) divergent slit: 0.6 mm; viii) Soller slit: 2.5°; ix) filter: K $\beta$  of Ni.

#### 2.2.1.5. X-ray fluorescence

The chemical analysis of the CCB was obtained from the x-ray fluorescence (FRX) assay in a RIX 2000 spectrometer of the RIGAKU brand, performed in the Geochemical Laboratory of the Federal University of Rio Grande do Sul (UFRGS), with Rh x-ray tube. In this research, quantitative analysis was carried out using the molten sample technique, with a calibration curve from rock standards and artificial standards for the majority of element found. The presence of volatiles was evaluated through gravimetric techniques.



**Figure 5:** Grinding process of the bamboo stalk ash.

### 2.2.1.6. Performance index with Portland cement at 28 days

The performance index with Portland cement was verified as prescribed in NBR 5752 [11]. This method evaluates the pozzolanicity of the materials from the simple compression test in mortars. Four mortars were prepared and mixed in a mechanical mixer, according to NBR 7215 [23], and described in Table 5. The use of admixture was dispensed.

After mixing, the mortars were submitted to consistency testing (Figure 6a) according to Annex B of the same standard. Four 50 x 100 mm cylindrical specimens were molded for each mortar (Figure 6b). After 28 days, the specimens were subjected to compression testing (Figure 7), according to NBR 7215 [23], in an EMIC DL200 testing machine, with a loading speed of 0.25 MPa/s. The performance index with Portland cement at 28 days was calculated for each of the mortars. For the material tested to be considered pozzolanic, this index should be greater than or equal to 90%, according to the physical requirements of NBR 12653 [24].

**Table 5:** Mortar composition for pozzolanicity evaluation of CCB.

| MORTAR     | CP II-F-32 (g) | CCB500 (g) | CCB600 (g) | CCB700 (g) | SAND (g) | WATER (g) |
|------------|----------------|------------|------------|------------|----------|-----------|
| IAP:REF    | 624.00         | –          | –          | –          | 1872.00  | 374.40    |
| IAP:CCB500 | 468.00         | 156.00     | –          | –          | 1872.00  | 374.40    |
| IAP:CCB600 | 468.00         | –          | 156.00     | –          | 1872.00  | 374.40    |
| IAP:CCB700 | 468.00         | –          | –          | 156.00     | 1872.00  | 374.40    |

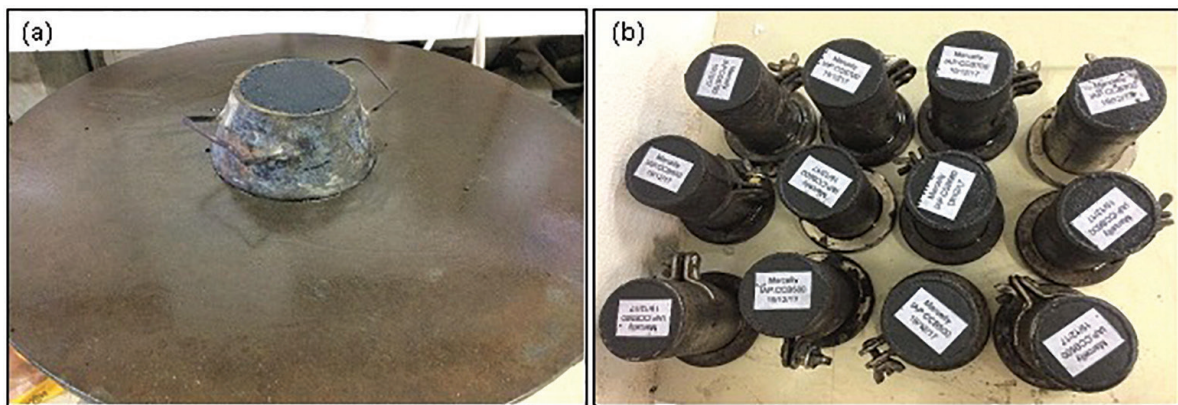


**Figure 6:** (a) Mortar consistency test; (b) Molds with mortars with CCB.



**Figure 7:** Mortar compression strength test.

### 2.2.2. Analysis of the hydration of cement partially replaced with bamboo ash

#### 2.2.2.1. Production of the pastes

The pastes were produced with Portland cement CP V-ARI and CCB at varying levels, according to Table 6. The water/binder ratio was 0.40 for all samples. The replacement levels were based on CP II-Z type cement, according to NBR 11578 [25]. On the date of the analyses, the samples (Figure 8a) were fragmented and ground (Figure 8b). The resulting powder was passed through a sieve of 0.075 mm and the passing material was stored and destined for the tests (Figure 8c).

#### 2.2.2.2. Pastes mineralogy

The produced pastes were submitted to XRD analysis at ages 28 and 56 days. The samples can be seen in Figure 9. The analysis was performed in the same equipment and conditions of the analyses in item 3.1.4.

**Table 6:** Cement and CCB600 contents in pastes.

| PASTES       | PCB0 | PCB6 | PCB10 | PCB14 |
|--------------|------|------|-------|-------|
| CCB (%)      | 0    | 6    | 10    | 14    |
| CP V-ARI (%) | 100  | 94   | 90    | 86    |

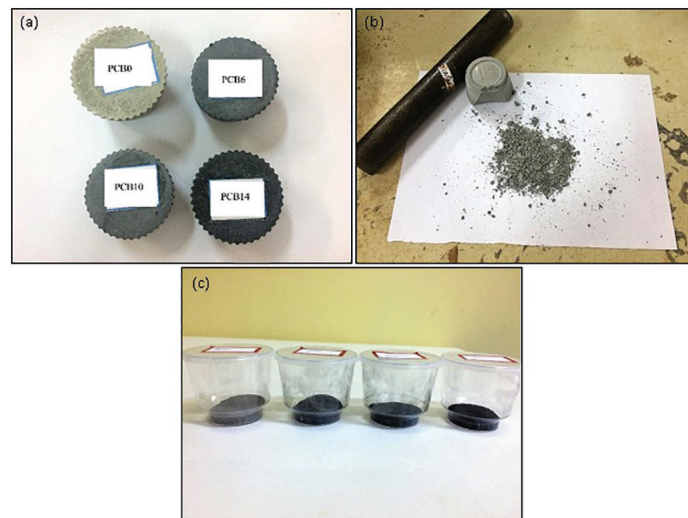


**Figure 8:** (a) Hydrated cement samples; (b) Sample fragmentation for tests; (c) Pulverized pastes for analysis.

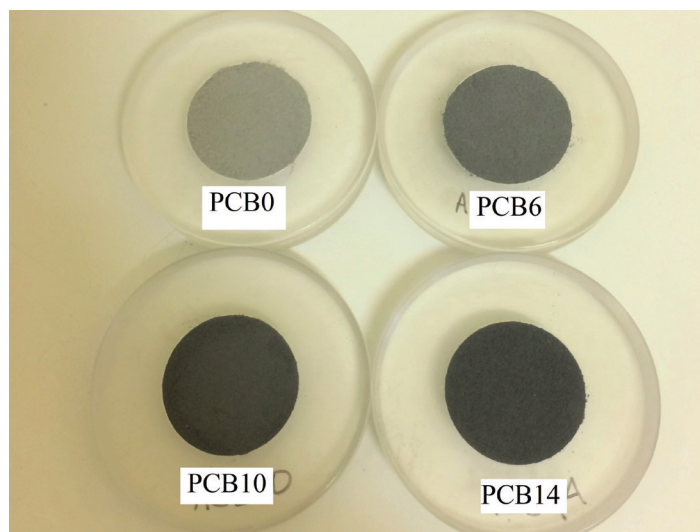


**Figure 9:** Samples of the pastes destined for X-ray diffraction.



### 2.2.2.3. Thermogravimetry of the hydrated pastes

The paste samples described above were analyzed at 56 days. The mass losses observed in the TG results occurred due to the dehydration of the hydration products of Portland cement. The test was performed in the Laboratory of Amazonian Oils, in the Guamá Science and Technology Park, and a Shimadzu thermobalance was used, with the following test conditions: i) alumina crucible; ii) temperature range: 20–1000°C; iii) rate: 10 °C/min; iv) nitrogen gas atmosphere; v) flow: 40 ml/min.

Thermogravimetric (TG) and its derived (DTG) curves were plotted. TG shows the sample mass variation, in percentage, in relation to temperature, while DTG is the derivative of TG in relation to time, in which the TG steps are replaced by peaks that delimit areas proportional to the sample mass variation.

### 2.2.3. Mortars with partial replacement of cement by bamboo ash

The last stage of the research consisted of the production of mortars with the same proportions of partial replacement of cement by CCB used in the pastes produced in the previous stage, based on the Portland cement compound, according to NBR 11578 [25]. The same CCB600 selected for the production of the pastes was also used. The mortars produced were analyzed for consistency in the fresh state and mechanical compressive strength. Finally, after the tests, fragments of the mortars were analyzed by SEM.

#### 2.2.3.1. Mortar mixture and consistency evaluation

The mortars (ACB – Bamboo brace mortar) were composed of Portland cement CP V-ARI and CCB in different proportions, according to Table 7; and sand and water in constant quantities, with the binder/sand ratio equal to 1:3 and the water/binder ratio, 0.55. The mixing procedure in a mechanical mixer, and the consistency test, on a table for consistency index, were performed according to NBR 7215 [23].

After mixing the mortars and determining the consistency index, 12 50 × 100 mm specimens were molded according to NBR 7215 [23] for each mortar to be submitted to compression testing at 3, 7 and 28 days (4 specimens for each age). Figure 10 shows a specimen of each mortar produced.

#### 2.2.3.2. Mechanical analysis – determination of compressive strength

According to NBR 7215 [23], the compressive strength test was performed on specimens molded from the previously mentioned mortars at 3, 7 and 28 days. The compressive strength test was performed in a universal hydraulic press model WAW – 1000C, with a maximum capacity of 100 tf and indicator division of 0.01 tf. Each specimen was positioned in the testing machine and centered on the loading axis, which was applied at a speed of 2 mm/min.

**Table 7:** Cement and CCB600 contents in the mortars.

| MORTARS      | ACB0 | ACB6 | ACB10 | ACB14 |
|--------------|------|------|-------|-------|
| CCB (%)      | 0    | 6    | 10    | 14    |
| CP V-ARI (%) | 100  | 94   | 90    | 86    |



**Figure 10:** Specimens of ACB0, ACB6, ACB10 and ACB14, from left to right.

### 2.2.3.3. Microstructure of mortars

The microstructure of the mortars was visualized by analysis with a TESCAN VEJA 3 LMU scanning electron microscope at the IFPA Metallurgy Laboratory. For this purpose, fragments were extracted from the mortar specimens and submitted to the compressive strength test at 28 days. The tested specimens were sectioned with a circular saw so that a cylindrical mortar section with approximately 0.5 cm in height was extracted. The extracted samples were submitted to a temperature of 100°C in an oven. The images generated in the SEM were not harmed by humidity and were later fragmented into small rectangular pieces, which were stored and destined for analysis. All samples were metalized with gold prior to the start of the analysis.

## 3. RESULTS AND DISCUSSION

### 3.1. Characterization of bamboo stalk ash

#### 3.1.1. Particle size analysis

The granulometric curves obtained from the laser granulometry analysis of the CCB500, CCB600, and CCB700 can be seen in Figures 11, 12 and 13, respectively. Curves were obtained for each grinding time to which the ash was submitted: 1, 2, 4, 6, and 8 hours.

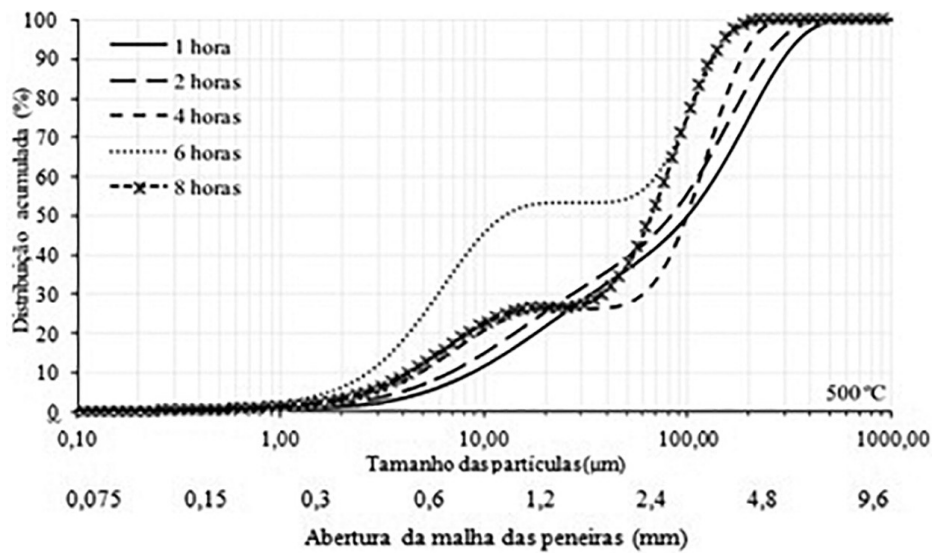


Figure 11: Particle size distribution curves for CCB500.

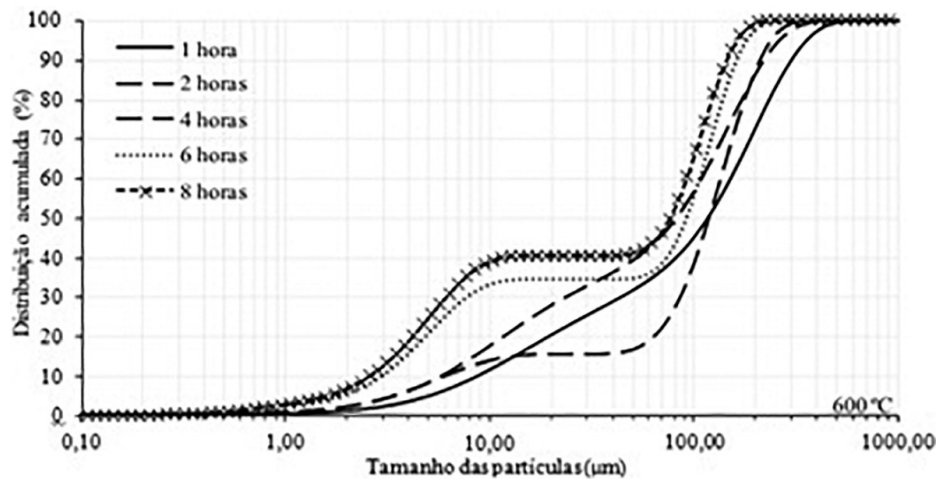


Figure 12: Particle size distribution curves of CCB600.

In general, the distribution of the curves shows that for the CCB600 and CCB700 ashes, the longer the grinding time, the smaller the grain sizes obtained. The CCB500, however, presented a finer material with 6 hours of grinding, to obtain with 8 hours of the process.

The average diameter (d50) of all samples was measured to evaluate the grain size (Table 8) quantitatively. It can be seen that grinding CCB500 for 6 hours was the most effective in decreasing the grain size, with an average diameter equal to 11.51  $\mu\text{m}$ . Grinding CCB500 for 8 hours resulted in a d50 equal to 62.35  $\mu\text{m}$ . The CCB600 and CCB700 presented the smallest average diameters with 8 hours of milling, 76.06  $\mu\text{m}$  and 56.45  $\mu\text{m}$ , respectively.

According to NBR 12653 [24], for a material to be considered pozzolanic, 80% of it must have a particle size less than 45  $\mu\text{m}$ . Therefore, only the CCB500 ground for 6 hours fits this standard since it has an average diameter of 11.51  $\mu\text{m}$ .

For the rest of the research, the ash ground at the times that presented the smallest average particle diameter was used: CCB500 ground for 6 hours, CCB600 ground for 8 hours and CCB700 ground for 8 hours.

### 3.1.2. Determination of gravity weight

The results of the gravity weight of the SCC, obtained by the average of two consecutive tests are shown in Table 9.

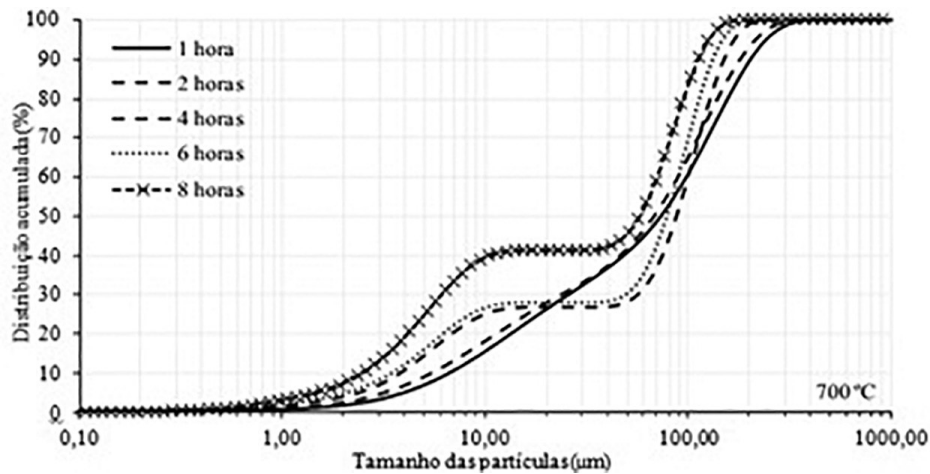


Figure 13: Particle size distribution curves for CCB700.

Table 8: Determination of the average diameter (d50) of the SCC after grinding.

| SAMPLE                   | 1h     | 2h    | 4h     | 6h           | 8h           |
|--------------------------|--------|-------|--------|--------------|--------------|
| CCB500 ( $\mu\text{m}$ ) | 92.78  | 76.06 | 92.78  | <b>11.51</b> | 62.35        |
| CCB600 ( $\mu\text{m}$ ) | 113.18 | 84.01 | 113.18 | 92.78        | <b>76.06</b> |
| CCB700 ( $\mu\text{m}$ ) | 68.87  | 68.87 | 84.01  | 76.06        | <b>56.45</b> |

Table 9: Gravity weight of the CCB.

| GREY   | SAMPLE   | m (g) | V <sub>1</sub> (cm <sup>3</sup> ) | V <sub>2</sub> (cm <sup>3</sup> ) | $\rho$ (g/cm <sup>3</sup> ) | $\rho_{\text{médio}}$ (g/cm <sup>3</sup> ) |
|--------|----------|-------|-----------------------------------|-----------------------------------|-----------------------------|--|
| CCB500 | CCB500-1 | 50.06 | 0.2                               | 24.0                              | 2.10                        | 2.11                                       |
|        | CCB500-2 | 50.13 | 0.3                               | 23.9                              | 2.12                        |  |
| CCB600 | CCB600-1 | 50.20 | 0.6                               | 23.5                              | 2.19                        | 2.18                                       |
|        | CCB600-2 | 50.05 | 0.2                               | 23.3                              | 2.17                        |  |
| CCB700 | CCB700-1 | 50.11 | 0.8                               | 23.8                              | 2.18                        | 2.20                                       |
|        | CCB700-2 | 50.02 | 0.9                               | 23.5                              | 2.21                        |  |

### 3.1.3. X-ray diffraction

From XRD results of the samples of CCB500 (Figure 14), CCB600 (Figure 15) and CCB700 (Figure 16), the presence of the minerals sylvite (KCl), calcite (CaCO<sub>3</sub>) and dolomite (CaMg(CO<sub>3</sub>)<sub>2</sub>) were identified, regardless of calcination temperature. The mineral that presented the highest peaks was sylvite, demonstrating that CCB can present large amounts of potassium oxide in the chemical composition. The diffractogram of CCB700 was the only one that showed a peak identified as quartz (SiO<sub>2</sub>), a crystalline form of silica.

The superposition of the CCB diffractograms (Figure 17) show that all the ashes present an amorphous hump between the 10° and 25° 2θ angles for all calcination temperatures. Its intensity decreases with the increase of the calcination temperature.

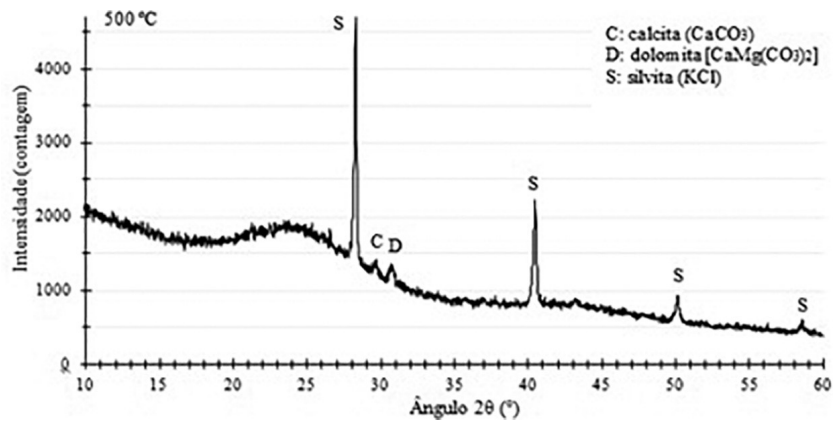


Figure 14: Diffractogram of CCB500.

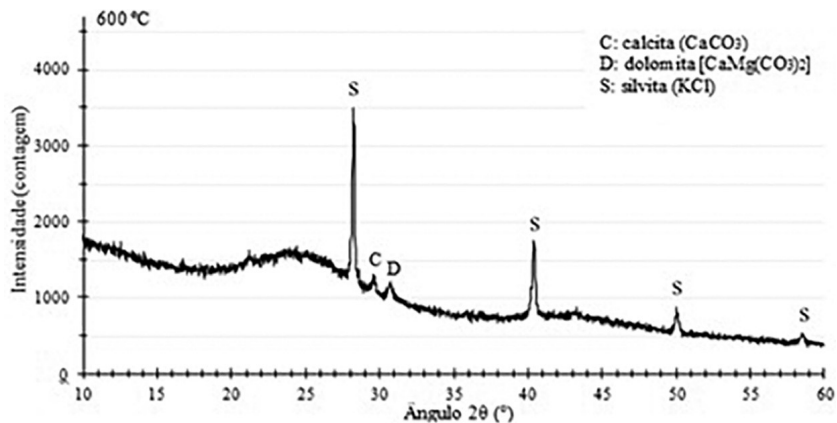


Figure 15: Difratogram from CCB600.

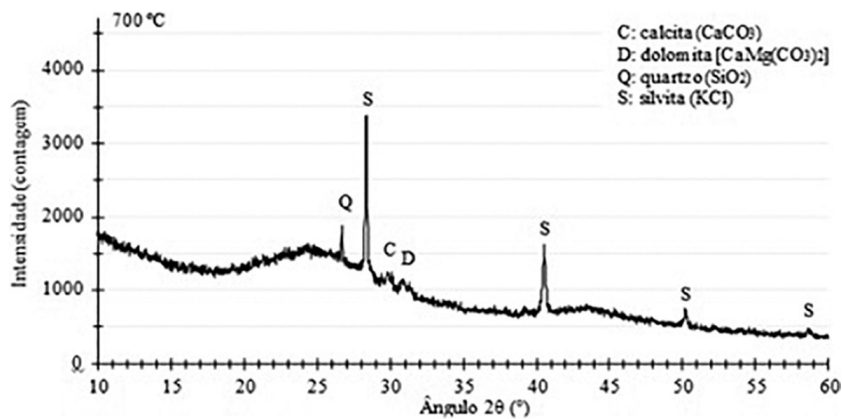


Figure 16: Diffractogram of CCB700.

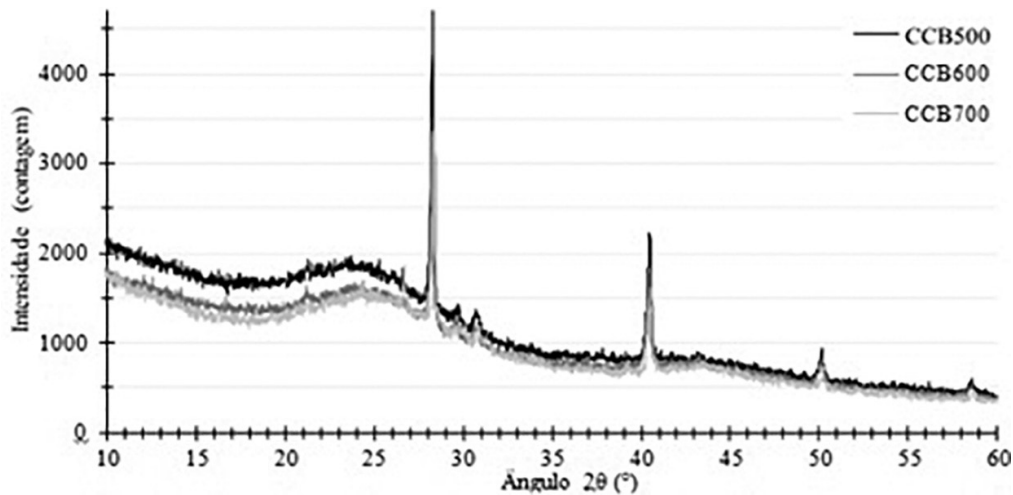


Figure 17: Overlapping diffractograms of CCB500, CCB600 and CCB700.

The XRD analysis allowed the determination of the crystalline mineral peaks present in the sample. All samples presented peaks of sylvite, calcite and dolomite, being the most expressive peaks of sylvite, a mineral composed by potassium and chlorine. An amorphous halo was also observed in all diffractograms, and from the superposition of the graphs, it was noted that the amorphous halo was more intense the lower the calcination temperature to which the ash had been submitted. The diffractogram of CCB700 was the only one that showed a peak of quartz, silica in crystalline form.

### 3.1.4. Chemical composition

The XRF analysis (Table 10) showed that CCB600 has a silica content of 12.25% (SiO<sub>2</sub>), refuting the hypothesis that ash from bamboo stalks is a silica-rich material.

The CCB does not meet some important chemical requirements of NBR 12653 [24], which determines the requirements for a material to be considered pozzolanic. Only the percentage of alkali available in Na<sub>2</sub>O meets the chemical requirement of the standard, which is a maximum of 1.5%; the CCB has 0.16%. According to the standard, the sum of SiO<sub>2</sub>, Al<sub>2</sub>O<sub>3</sub> and Fe<sub>2</sub>O<sub>3</sub> should be equal to at least 50%; CCB presented 12.93% in the sum of these compounds. The loss on ignition must not be greater than or equal to 10%; the CCB presented 27.38% loss on ignition.

### 3.1.5. Performance index with Portland cement at 28 days

The results of individual compressive strength of specimens, average compressive strength of mortars evaluated, relative deviations and consistency index are shown in Table 11. The PSI: CCB500 presented the lowest consistency index, followed by PSI: CCB700 and PSI: CCB600, respectively. The IAP: REF presented the highest consistency index, 0.5cm higher than the IAP: CCB600.

The performance indices with Portland cement at 28 days can be seen in Figure 18. According to NBR 12653 [24], this index should be greater than 90% for the evaluated material to be considered pozzolanic. The mortar with CCB600 was the only one that exceeded this value, with an index of 93.51%.

Given the results obtained in the stage of characterization of the CCB, it was decided to continue the research using only the sample of bamboo stem ash calcined at 600°C (CCB600), because when used in mortar, the CCB600 guaranteed 93.51% of the compressive strength of the reference mortar, despite not meeting the chemical requirements of NBR 12653 [24]. Thus, further research on the use of CCB600 becomes relevant.

Table 10: Chemical composition of CCB600.

| SiO <sub>2</sub> | Al <sub>2</sub> O <sub>3</sub> | TiO <sub>2</sub> | Fe <sub>2</sub> O <sub>3</sub> | MnO   | MgO   | CaO   | Na <sub>2</sub> O | K <sub>2</sub> O | P <sub>2</sub> O <sub>5</sub> | PF <sup>1</sup> |
|------------------|--------------------------------|------------------|--------------------------------|-------|-------|-------|-------------------|------------------|-------------------------------|-----------------|
| 12.25%           | 0.56%                          | 0.02%            | 0.12%                          | 0.08% | 1.90% | 0.92% | 0.16%             | 50.42%           | 5.45%                         | 27.38%          |

<sup>1</sup>loss on ignition.

**Table 11:** Consistency and average mortar strength.

| MORTAR     | SAMPLE | COMPRESSIVE STRENGTH (MPa) | MAX. RELATIVE DEVIATION | CONSISTENCY INDEX (cm) | AVERAGE COMPRESSION STRENGTH (MPa) |
|------------|--------|----------------------------|-------------------------|------------------------|------------------------------------|
| IAP:REF    | REF-01 | 17.05                      | 3.15%                   | 23.0                   | 17.61                              |
|            | REF-02 | 18.53                      | -5.25%                  |                        |                                    |
|            | REF-03 | 17.40                      | 1.16%                   |                        |                                    |
|            | REF-04 | 17.44                      | 0.94%                   |                        |                                    |
| IAP:CCB500 | 500-01 | 13.42                      | -0.39%                  | 21.5                   | 13.37                              |
|            | 500-02 | 13.71                      | -2.56%                  |                        |                                    |
|            | 500-03 | 13.37                      | -0.02%                  |                        |                                    |
|            | 500-04 | 12.97                      | 2.97%                   |                        |                                    |
| IAP:CCB600 | 600-01 | 16.02                      | 2.69%                   | 22.5                   | 16.46                              |
|            | 600-02 | 16.41                      | 0.32%                   |                        |                                    |
|            | 600-03 | 16.71                      | -1.50%                  |                        |                                    |
|            | 600-04 | 16.71                      | -1.50%                  |                        |                                    |
| IAP:CCB700 | 700-01 | 15.23                      | -2.20%                  | 22.0                   | 14.90                              |
|            | 700-02 | 14.60                      | 2.03%                   |                        |                                    |
|            | 700-03 | 14.79                      | 0.75%                   |                        |                                    |
|            | 700-04 | 14.99                      | -0.59%                  |                        |                                    |

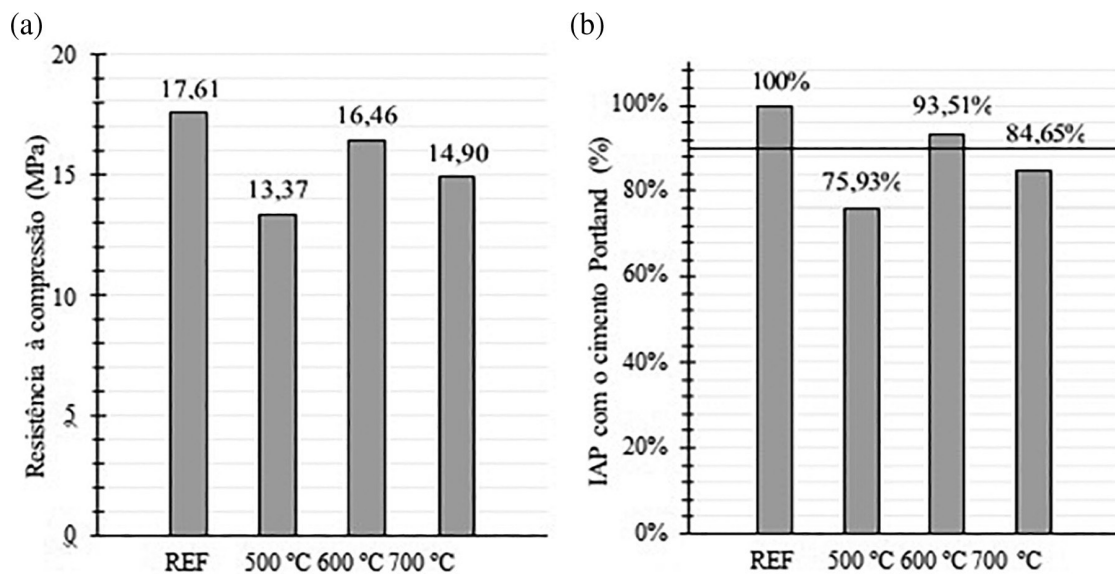


**Figure 18:** (a) Compressive strength; (b) Performance index with Portland cement.

### 3.2. Analysis of the hydration of cement partially replaced with bamboo ash

#### 3.2.1. Mineralogy of hydrated pastes

The diffractograms generated from the XRD analysis of PCB0, PCB6, PCB10 and PCB14, are arranged in Figures 19, 20, 21 and 22, respectively. Where \* are identification of the peaks of Portlandite.

It was observed in all pastes the presence of the anhydrous phases of Portland cement, bellite (C2S), both at 28 and 56 days of age. There were not identified, in turn, peaks of alite (C3S), since this compound is

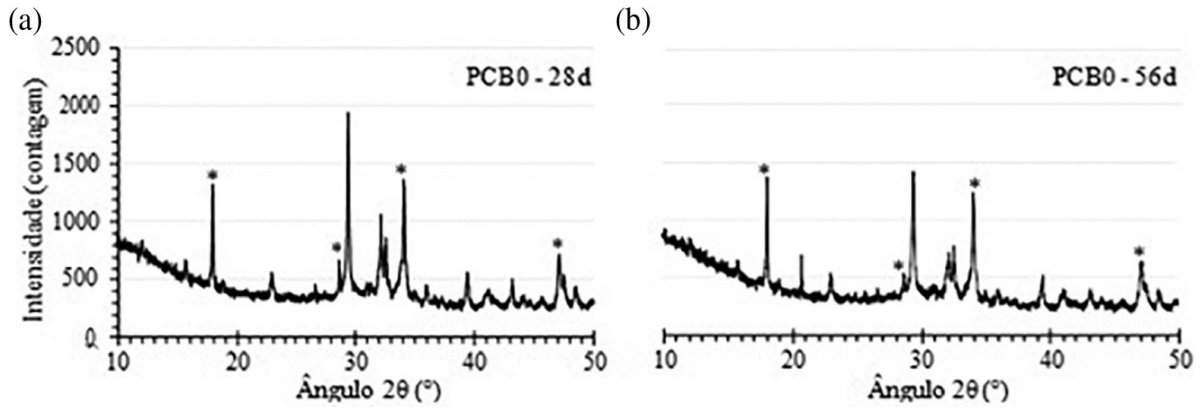


Figure 19: Diffractograms of PCB0 (a) 28 days; (b) 56 days.

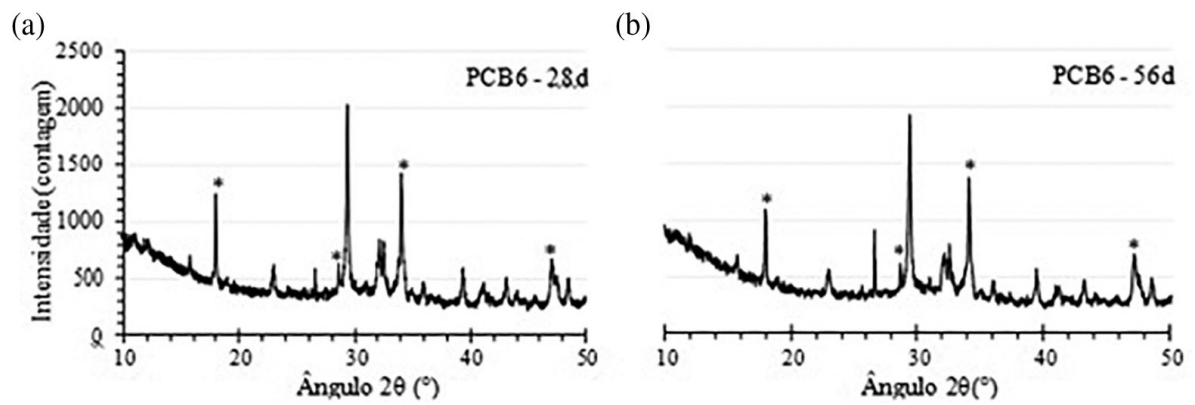


Figure 20: Diffractograms of PCB6 (a) 28 days; (b) 56 days.

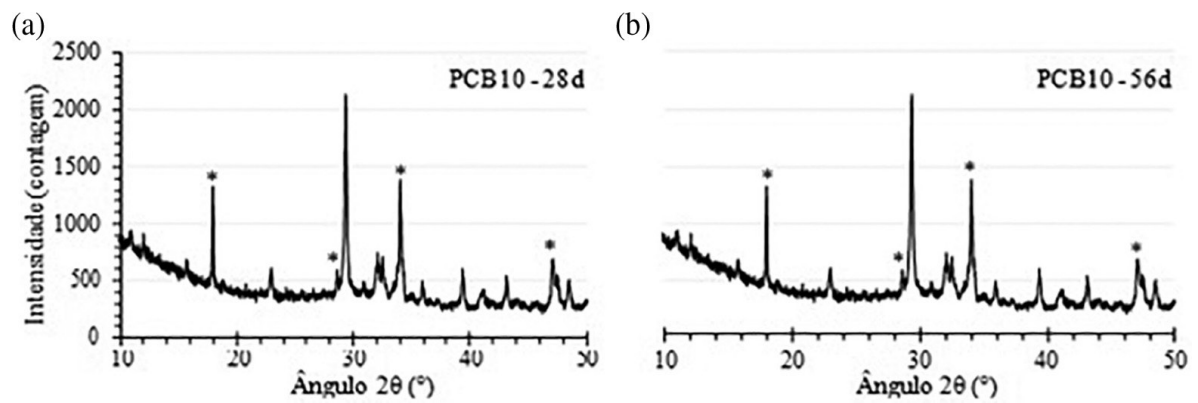


Figure 21: Diffractograms of PCB10 (a) 28 days; (b) 56 days.

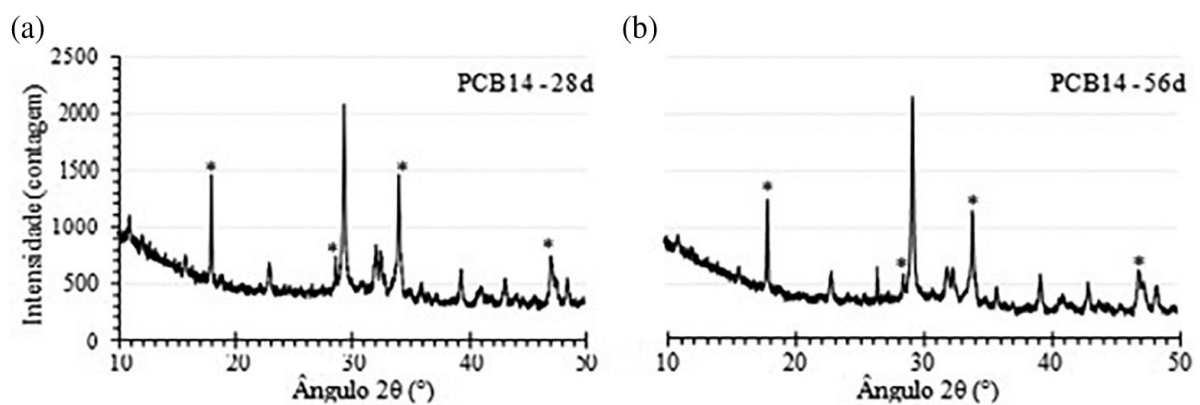


Figure 22: Diffractograms of PCB14 (a) 28 days; (b) 56 days.

much more reactive than the C2S, and the first, under normal temperature conditions, is usually 50% hydrated in 3 days and 80% at 28 days.

Ettringite is usually one of the first compounds to precipitate during cement hydration [1]. It was identified in all diffractograms. In order to be able to evaluate the intensity of the ettringite peak comparatively, the detail of the peak at  $15.73^{\circ}2\theta$  of all samples was superimposed at 28 (Figure 23a) and 56 days (Figure 23b). No significant distinction was observed in the behavior of pastes with different CCB contents with respect to ettringite formation and the difference between ages was practically imperceptible.

The detail of the calcite peak at  $29.4^{\circ}2\theta$  is illustrated in Figure 24 for the two ages of analysis. It can be seen that at 28 days the peak intensity is quite similar among all the samples. However, over time, the PCB0 sample showed a decrease in the intensity of this peak, while in the other samples, the peak remained practically unchanged.

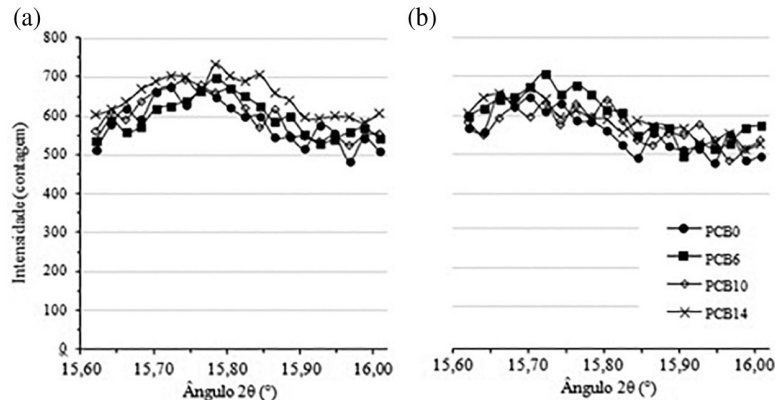


Figure 23: Detail of the ettringite peak at  $15.73^{\circ}2\theta$  (a) 28 days; (b) 56 days.

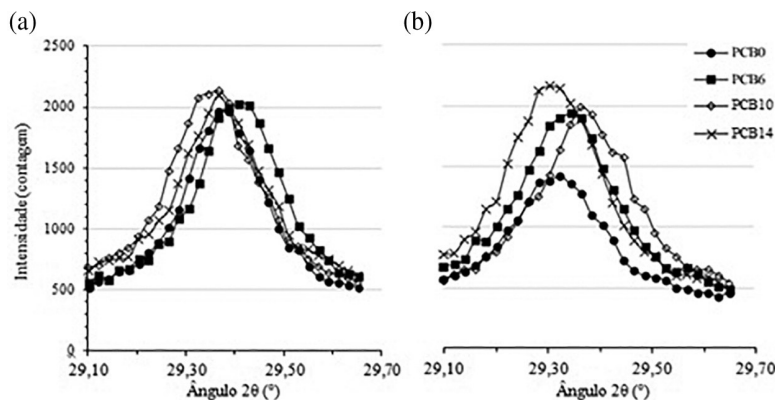


Figure 24: Detail of the calcite peak at  $29.4^{\circ}2\theta$  (a) 28 days; (b) 56 days.

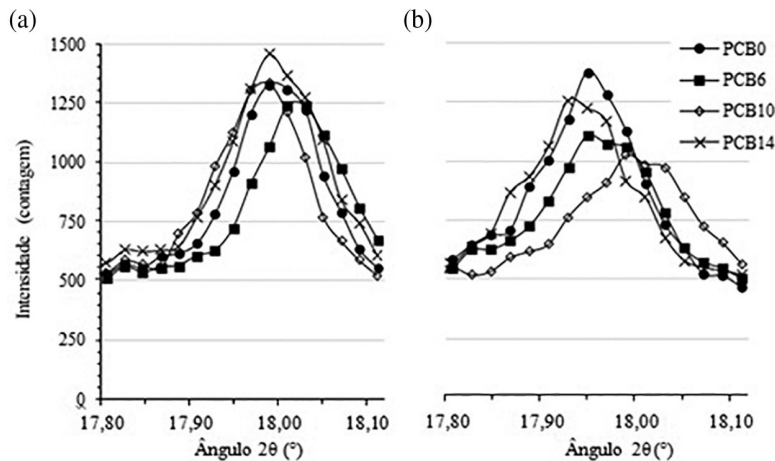


Figure 25: Detail of the portlandite peak at  $18.1^{\circ}2\theta$  (a) 28 days; (b) 56 days.



Figure 25, which illustrates in detail overlapping peaks of portlandite at 18.1°2θ of all samples. It is visualized at 28 days that all samples presented peaks with practically the same intensity. At 56 days, samples PCB6, PCB10 and PCB14 showed a decrease in the peaks' intensity, while that of sample PCB0 was slightly increased. The PCB10 sample presented lower peak intensity, on the order of 1000, while the intensity of the PCB0 peak was close to 1350. It is known that this phenomenon is common in the incorporation of pozzolans into cement, which consumes calcium hydroxide in the presence of water and forms more resistant materials. However, the CCB incorporated in the pastes does not meet the chemical requirements of NBR 12653 [24] to be considered pozzolanic.

**3.2.2. Thermogravimetry of the hydrated pastes**

TG and DTG curves of PCB0, PCB6, PCB10 and PC14 samples showed typical behavior of hydrated cement pastes, with the identification of three endothermic reactions in distinct and well-defined temperature ranges (Table 12), generating peaks of mass loss. The temperature ranges were defined as I, II and III. I) referring to the water evaporation reaction of the paste hydrated compounds, such as ettringite and hydrated calcium silicates and aluminates; II) refers to the decomposition of calcium hydroxide; III) to the decomposition of carbonate phases, as proposed by EL-JAZAIRI and ILLSTON [26] apud RODIER *et al.* [21].

The graphs obtained from the thermogravimetric analysis, containing the TG and DTG curves of samples PCB0, PCB6, PCB10 and PCB14, at 56 days, can be seen in Figures 26, 27, 28 and 29, respectively.

**Table 12:** Decomposition temperature ranges of the hydration products of the pastes.

| SAMPLES | C-S-H + C-A-H + ETRINGITA (°C) | Ca(OH) <sub>2</sub> (°C) | CaCO <sub>3</sub> (°C) |
|---------|--------------------------------|--------------------------|------------------------|
|         | I                              | II                       | III                    |
| PCB0    | 44–113                         | 433–445                  | 667–709                |
| PCB6    | 36–118                         | 436–457                  | 501–715                |
| PCB10   | 50–127                         | 432–452                  | 631–914                |
| PCB14   | 53–116                         | 431–448                  | 633–945                |

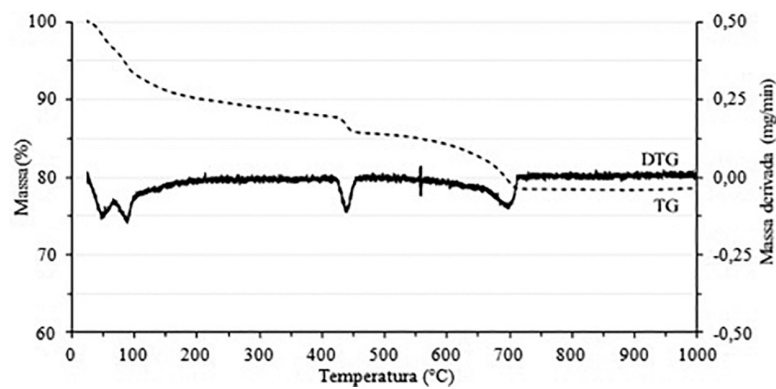


**Figure 26:** TG/DTG of PCB0 (56 days).

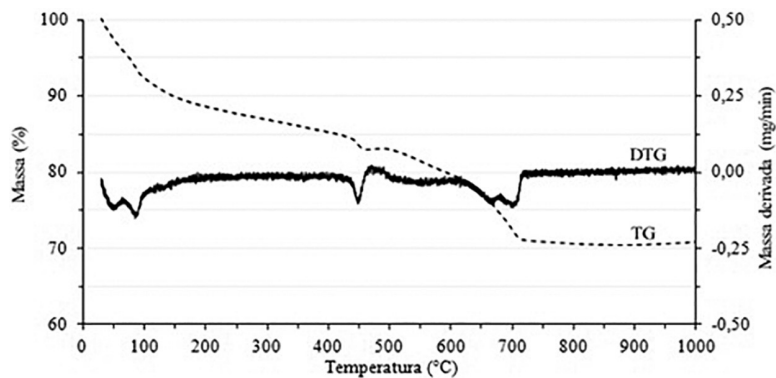


**Figure 27:** TG/DTG of PCB6 (56 days).

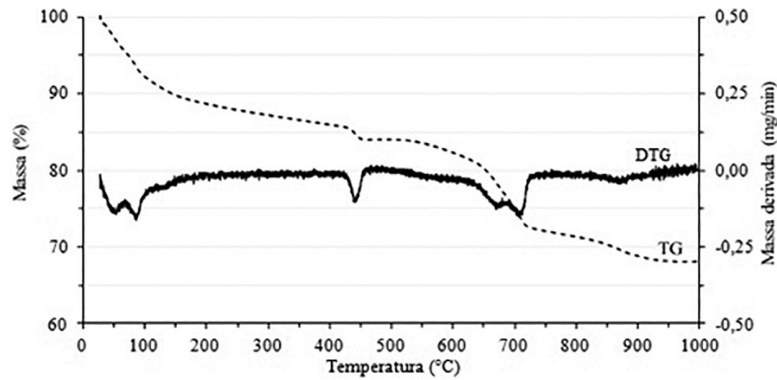


Figure 28: TG/DTG of PCB10 (56 days).

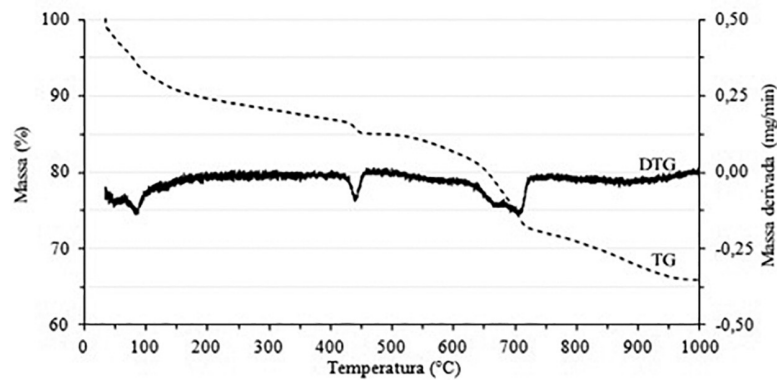


Figure 29: TG/DTG of PCB14 (56 days).

Table 13: Loss of mass of the pastes by temperature range.

| SAMPLES | RANGE I | RANGE II | RANGE III |
|---------|---------|----------|-----------|
| PCB0    | 10.49%  | 4.36%    | 6.90%     |
| PCB6    | 12.67%  | 4.33%    | 12.53%    |
| PCB10   | 14.17%  | 1.74%    | 15.75%    |
| PCB14   | 13.12%  | 1.77%    | 19.04%    |

In all samples, the temperature range I presented two peaks of mass loss in DTG. The first is related to mass loss by evaporable water. While the second is interlamellar water from hydrated phases such as ettringite, C-S-H and/or C-A-S-H. A subtle decrease in the DTG peak was identified in range II, demonstrating a possible decrease in the amount of calcium hydroxide present in the samples with the increase in CCB content. In range III, PCB0 and PCB6 samples have a mass constancy around 750°C, while PCB10 and PCB14 pastes, small amounts of mass are lost between 750°C and 950°C. For these variations to be quantified, the mass loss, in percent, of each temperature range was determined (Table 13).

An increase in mass loss occurred in range I with the addition of CCB in the pastes, indicating a greater amount of evaporable water bound to the hydrated compounds. In range II of temperature, the effect was inverse; the addition of the ashes caused a lower mass loss referring to the decomposition of calcium hydroxide. PCB6 suffered a mass loss in range II almost equal to that of PCB0 (4.33% and 4.36%, respectively). PCB10 and PCB14 showed a loss quite close to each other (1.74% and 1.77%, respectively) and lower than the other two samples. In range III, the higher the amount of CCB, the higher the mass loss related to the decomposition of carbonate phases due to the carbon present in the ash.

MORAES [27], when studying the hydration of pastes with 15% replacement of Portland cement by ash from sugar cane leaf, found results very close to those of this study for mass loss due to dehydration of calcium hydroxide. At 28 days, the control sample lost 2.92% mass, while the sample with replacement lost 1.53%. At 60 days, the value of the control sample increased to 3.20%, while the sample with the substitution was increased to only 1.60%

From the mass loss in temperature range III, all the evaluated pastes contain carbonate phases. However, the amount of mass loss in range III increases with the increase in CCB content. The ACB6 paste already presents practically twice the mass loss, in this temperature range, concerning ACB0. The chemical composition of the ashes, with a large amount of potassium oxide, an alkali, may have facilitated the occurrence of the carbonation phenomenon. The considerable percentage of ash loss on ignition may also have been responsible for increased carbonate content.

According to POSSAN [28], carbonation occurs by the reaction of CO<sub>2</sub> with hydroxides, especially calcium hydroxide, which is found in larger quantities in the presence of moisture. Calcium and potassium hydroxides also stand out. Consequently, carbonation decreases the pH of mixtures. In reinforced concrete, it can reduce the passive protection of reinforcement and decrease the structure’s durability, which becomes vulnerable to corrosion.

Finally, the amount of calcium hydroxide present in the pastes was calculated from the mass loss in temperature range II (Table 14). The decrease in calcium hydroxide in the pastes was very significant in the samples, with 10% and 14% of CCB in the reference sample. The sample with 6% presented practically the same amount of calcium hydroxide as the PCB0.

### 3.3. Mortars with partial replacement of cement by bamboo ash

#### 3.3.1. Analysis in the fresh state – consistency

The water/cement ratio was constant in all mortars produced. The use of a superplasticizer was unnecessary because from the determination of the normal consistency index, according to NBR 7215 [23], all mortars produced presented practically the same consistency (Table 15). According to NBR 5752 [11], the consistency index of mortars with substitution can vary up to ± 10 mm from the index of the reference mortar. Figure 30 illustrates the appearance of the mortars after the test.

**Table 14:** Amount of calcium hydroxide in the pastes.

| PCB0   | PCB6   | PCB10 | PCB14 |
|--------|--------|-------|-------|
| 17.92% | 17.80% | 7.15% | 7.25% |

**Table 15:** Mortar consistency index.

| MORTAR | MEASURE 1 (mm) | MEASURE 2 (mm) | MEASURE (mm) |
|--------|----------------|----------------|--------------|
| ACB0   | 225            | 228            | 227          |
| ACB6   | 223            | 224            | 224          |
| ACB10  | 226            | 228            | 227          |
| ACB14  | 227            | 228            | 228          |



**Figure 30:** Determination of the consistency index (a) ACB0; (b) ACB6; (c) ACB10; (d) CBA14.

### 3.3.2. Mechanical analysis – determination of compressive strength

The compressive strength results of the mortars ACB0, ACB6, ACB10, and ACB14 at 3, 7 and 28 days are presented in Figure 31. The appearance of the mortars after the test at 28 days is shown in Figure 32. In general, the compressive strength increased at longer ages. The partial replacement of Portland cement with bamboo stalks ash calcined at 600°C increased the compressive strength of mortars due to the physical and chemical effects. The filler effect and particle packing with the addition of fine material concomitantly can explain that. The chemical effect is based on the reaction of the small content of amorphous silica present in CCB during hydration of Portland cement, consuming calcium hydroxide and forming more resistant hydrated products, as tended the result of thermogravimetric and XRD analysis.

The statistical analysis showed a significant difference between all mortars evaluated at 3 days. CBA6 presented the highest result, 21.96 MPa, and CBA0, without the addition of CCB, the lowest, 15.59 MPa. There was an increase of approximately 41% in compressive strength of the mortar, with 6% of CCB higher than reference mortar. However, by increasing the substitution content, the increase in strength at 3 days decreases. The CBA10 had an increase of 31.49% and CBA14, of 23.80%, both higher than CBA0.

At 7 days, the behavior of the mortars' compressive strength remained similar to that of 3 days, increasing proportionally due to the age in each mortar. All mortars showed significant differences among themselves. The increase in compressive strength of PCB6 about PCB0 was around 36%. CBA10 had an increase of 27.98% and CBA14, of 15.18%, about CBA0.

At 28 days, all mortars with CCB (ACB6, ACB10 and ACB14) showed between 10 and 15% increase in relation to the compressive strength of the reference mortar (ACB0). By subjecting only the mortars with CCB to statistical analysis, it became evident that at 28 days, the compressive strength of ACB6, ACB10 and ACB14 is equal (Figure 33).

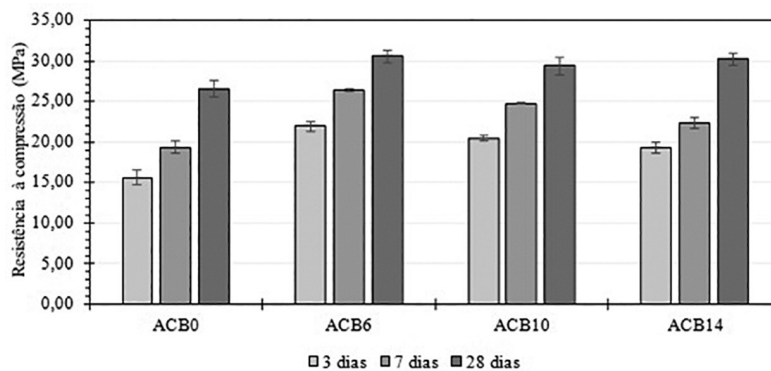


Figure 31: Result of the mortar compressive strength.

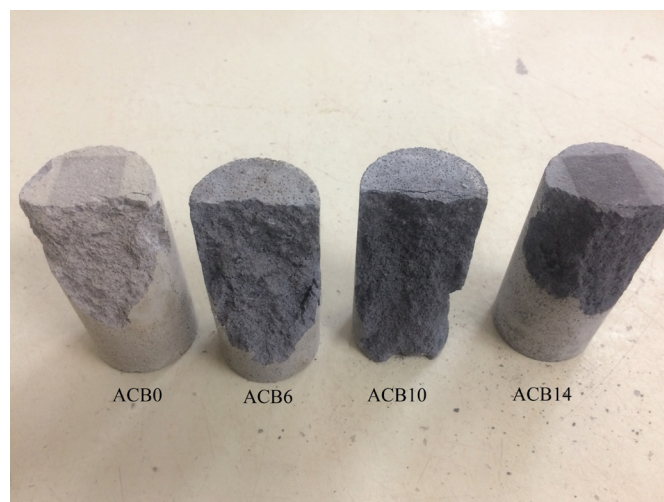


Figure 32: Mortar fracture after compressive strength (28 days).

The mineralogical and thermogravimetric analyses showed a decrease in the concentration of calcium hydroxide. However, the CCB evaluated in this research does not have the necessary chemical composition to be considered pozzolanic and reactive. Moreover, the increase in compressive strength of mortars with CCB can also be attributed to the physical effect of filling voids, densifying the structure from the filler effect by the non-reactive part of the CCB.

### 3.3.3. Microstructure of mortars

Images were generated from secondary and backscattered electron beams with 100x magnification of all mortars to compare the microstructural appearance of their surfaces. Figures 34, 35, 36 and 37 correspond to the images generated from samples ACB0, ACB6, ACB10 and ACB14, respectively.

Some images have micro-cracks since all samples come from mortar compressive strength samples. Note that the samples were extracted from the bases of the specimens, which remained intact to the naked eye. From the images on the right, generated by backscattered electron beams, one can see more concentrated areas with darker coloration in the ACB0 and ACB6, while the samples ACB10 and ACB14 present homogeneous coloration. In the images generated by backscattered electrons, the lighter the color illustrated, the denser the component of the sample.

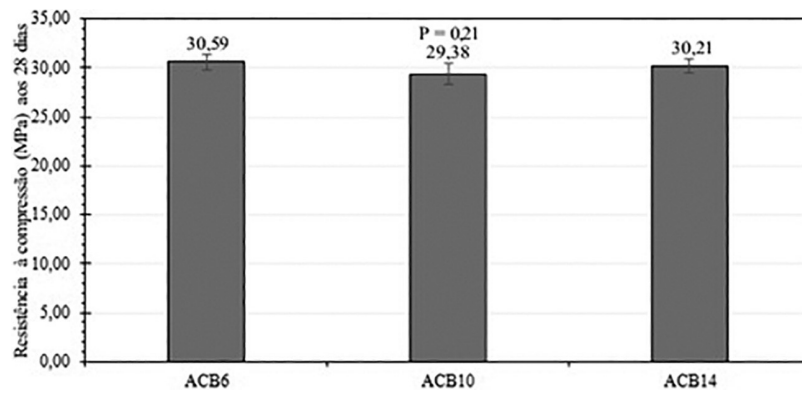


**Figure 33:** Result of compressive strength of mortars with CCB at 28 days (n = 4, significant variance when  $P < 0.05$ . ANOVA test, Tukey).

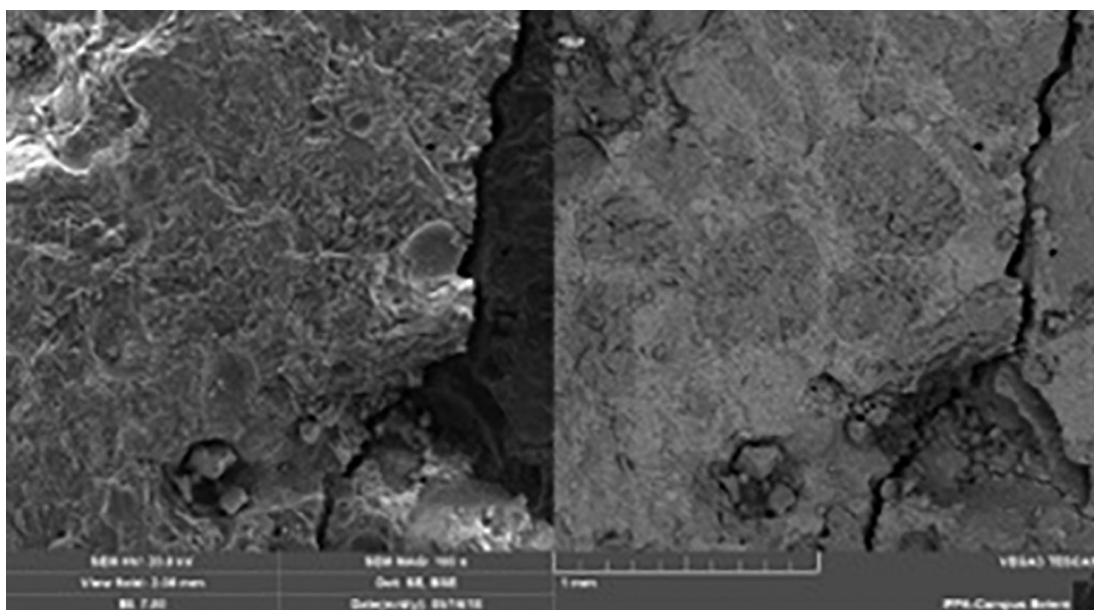


**Figure 34:** Surface of CBA0 magnified 100x.

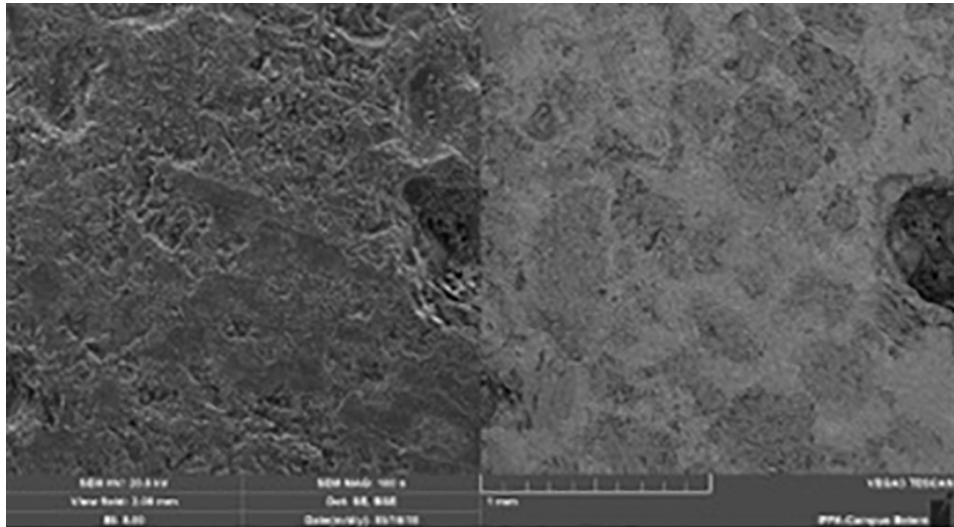


Figure 35: Surface of CBA6 magnified 100x.

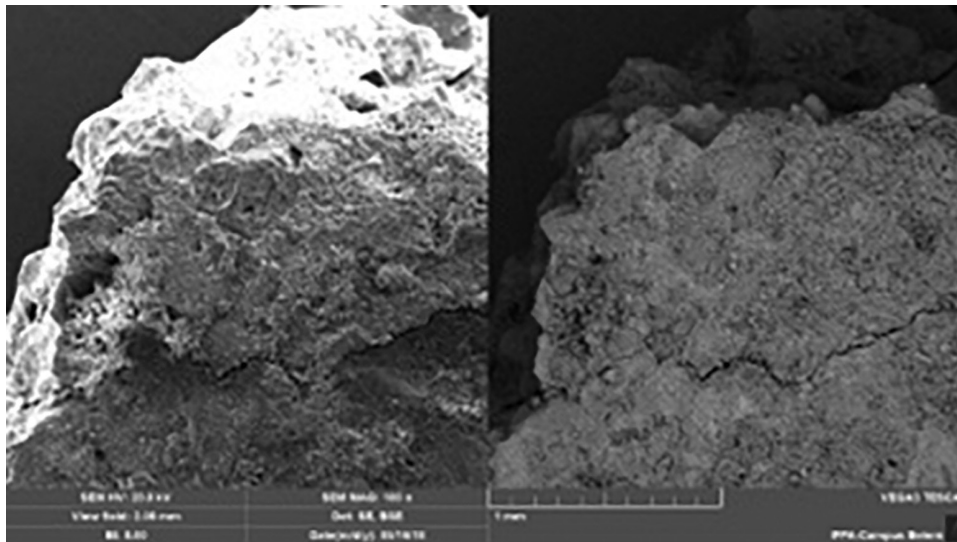


Figure 36: Surface of CBA10 magnified 100x.

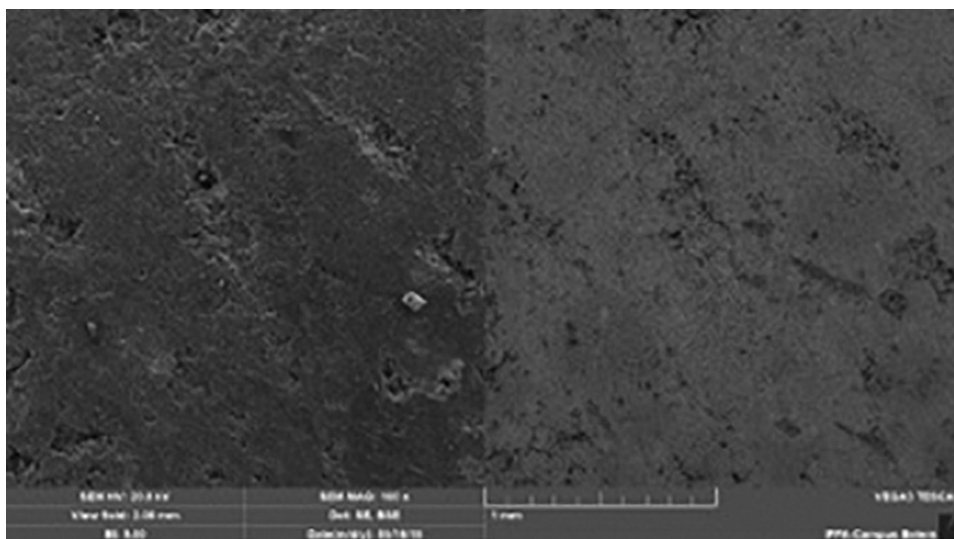


Figure 37: Surface of CBA14 magnified 100x.

#### 4. CONCLUSIONS

The first step was to characterize the bamboo stalks ashes from three calcination temperatures (500°C, 600°C and 700°C). The results showed that the ashes are not classified as pozzolanic material because they do not meet the chemical requirements of the standard.

The granulometric analysis defined that the CCB500 obtained the smallest average diameter from grinding for 6 hours, while the CCB600 and CCB700 for 8 hours. The particle size distribution curves for the chosen times characterized the distribution of the samples as discontinuous, i.e., they have tiny and other very large particles, with an absence of intermediate sizes. The ash's gravity weight of the underwent a slight increase with increasing calcination temperature and remained between 2.11 g/cm<sup>3</sup> and 2.20 g/cm<sup>3</sup>.

XRD analysis concluded the presence of amorphous silica in samples CCB500 and CCB600 from 700°C. During the calcination of the material, this silica tends to crystallize in the form of quartz. In its chemical composition, the CCB presents an amount of SiO<sub>2</sub>, Al<sub>2</sub>O<sub>3</sub> and Fe<sub>2</sub>O<sub>3</sub> much lower than the chemical requirement of NBR 12653 [24]; thus it is considered pozzolanic. According to the FRX analysis, the CCB has 12.93% of these oxides. Moreover, the CCB showed a high loss on ignition, greater than 20%, while the standard above requires a maximum limit of 10%. The chemical analysis of the CCB also showed a large amount of potassium 50.42%, one of the alkalis that can cause damage in cementitious matrices.

The performance index with Portland cement at 28 days is one of the physical requirements of NBR 12653 [24] and despite not meeting the chemical requirements of the same standard, CCB600 showed an index of 93.51%, higher than the minimum limit of the standard, which is 90%. The rates of CCB500 and CCB700 were respectively 75, 93% and 84.65%.

From characterization and physical requirements, it was decided to perform a further investigation on the properties of the bamboo stalks ash calcined at 600°C (CCB600) when inserted into Portland cement matrices as a partial replacement of the binder. This choice was also based on two aspects. First, the mineralogy of the ash showed a tendency of crystallization of amorphous silica in the form of quartz from 700°C. Then, the performance index with Portland cement at 28 days allowed verifying that the CCB600 guaranteed 93.51% of the compressive strength of the reference mortar, even replacing 25% of Portland cement, making relevant a continuity of studies.

The study also evaluated the hydration of cement partially replaced by bamboo ash. For this purpose, cement pastes were evaluated with binder substitution contents by CCB600 based on the composite Portland cement, according to NBR 11578 [25]: 0%, 6%, 10% and 14%.

From the XRD of the pastes hydrated at 28 and 56 days, it was possible to compare the intensity of the prominent mineral peaks: ettringite at 15.73°2θ, calcite at 29.4°2θ and portlandite at 18.1°2θ. The incorporation of ash into the mixtures caused no effects on the ettringite peak at both ages evaluated. The intensity of the calcite peak, on the other hand, remained the same for all samples at 28 days. However, at 56 days, the sample with 0% CCB showed less intensity than those with CCB. Finally, it was evaluated that the intensity of portlandite at 28 days was practically the same in all samples. However, at 56 days, the sample with 0% CCB slightly increased the peak intensity, while all samples with CCB had a decrease. The sample with 10% CCB showed lower peak intensity, on the order of 1000, while the peak intensity of the reference sample was close to 1350. This phenomenon is expected to incorporate pozzolans into cement, which consume calcium hydroxide in the presence of water and form more resistant materials. However, the CCB incorporated into the pastes does not meet the chemical requirements of NBR 12653 [24] to be considered pozzolanic.

From the decomposition of calcium hydroxide and decomposition of carbonate phases in different temperature ranges (seen in TG results), it was to quantify the mass loss by dehydration of hydration products (C-S-H, C-A-S-H and ettringite) at 56 days. The incorporation of ash increased the mass loss by dehydration of the hydration products and by decomposition of the carbonate phases. However, the amount of calcium hydroxide tended to decrease with ash incorporation. Confirming what was seen from the XRD analysis of the pastes, the sample with 10% of cement replacement by CCB presented the lowest amount of calcium hydroxide among the pastes. However, from this analysis, the incorporation of ash significantly increased the number of carbonate phases in the mixture, which may have caused the carbonation phenomenon, which can cause damage to reinforced concrete structures. A large number of alkalis may have facilitated the carbonation in the chemical composition of ash. The increase of carbonatic phases can also be explained by the high loss on ignition of ash.

The last stage of the work consisted of evaluating mortars with partial replacement of Portland cement by CCB. In the fresh state, the incorporation of CCB in the mortars did not cause damage to the consistency. All mortars presented practically the same consistency in the fresh state. In the hardened state, the influence of the incorporation of CCB in the mechanical resistance of mortars was evaluated. At 3 and 7 days, the samples

with CCB showed higher strengths than the reference sample, and the mortar with lower substitution content (6%) reached the highest strength. At 28 days, all mortars with CCB reached equal resistance, according to the statistical tests applied, and higher than the reference mortar. The increase in strength with the incorporation of ash was in the order of 15%.

From the microstructural analysis of the mortars, after the rupture in the compressive strength test, it was possible to visualize the appearance of the surface of the samples, and it was found that the samples with 10% and 14% substitution presented a denser surface, as visualized in the images with 100x magnitude, than the reference samples and those with 6% CCB.

## 5. BIBLIOGRAPHY

- [1] MEHTA, P.K., MONTEIRO, P.J.M., *Concrete: microstructure, properties, and materials*, 3 ed., Berkeley, McGraw-Hill, 2008.
- [2] MOIR, G., “Advanced concrete technology: constituent materials”, In: Newman, J., Choo, B.S. (eds), *Cements*, Oxford, Elsevier, 2003.
- [3] CORREIA, V.C., “*Produção e caracterização de polpa organossolve de bambu para reforço de matrizes cimentícias*”, M.Sc. Thesis, Universidade de São Paulo, Pirassununga, 2011.
- [4] FILGUEIRAS, T.S., VIANA, P.L., “Bambus brasileiros: morfologia, taxonomia, distribuição e conservação.” In: P. M. Drumond, G. Wiedman (eds), *Bambus no Brasil: da biologia à tecnologia*, Rio de Janeiro, ICH, pp. 10–27, 2017.
- [5] GUARNETTI, R.L., “*Cogeração de eletricidade utilizando bambu no Brasil: aspectos técnicos, econômicos e ambientais*”, D.Sc. Thesis, Universidade de São Paulo, São Paulo, 2013.
- [6] DEPARTMENT OF ECOLOGY, EVOLUTION AND ORGANISMAL BIOLOGY, “*Distribuição geográfica dos bambus lenhosos no mundo*”, <https://www.eeob.iastate.edu/research/bamboo/maps/world-total-woody.gif>, accessed in February 2018.
- [7] GUILHERME, D.O., RIBEIRO, N.P., CEREDA, M.P., “Cultivo, manejo e colheita do bambu”, In: P.M. Drumond, G. Wiedman (eds), *Bambus no Brasil: da biologia à tecnologia*, Rio de Janeiro, ICH, pp. 28–41, 2017.
- [8] TEIXEIRA, A.A., “*Painéis de bambu para habitação econômica: Avaliação do desempenho de painéis revestidos com argamassa*”, M.Sc. Thesis, Universidade de Brasília, Brasília, 2006.
- [9] MOGNON, F., SANQUETTA, C.R., CORTE, A.P.D., *et al.*, “Bambu, uma alternativa para o sequestro de carbono,” In: P.M. Drumond, G. Wiedman (eds), *Bambus no Brasil: da biologia à tecnologia*, Rio de Janeiro, ICH, pp. 28–41, 2017.
- [10] ARAGÃO, G.H., “*Estudo comparativo das características das malhas fabricadas com fibras de viscosa e de viscosa de bambu*”, M.Sc. Thesis, Universidade de São Paulo, São Paulo, 2015.
- [11] ASSOCIAÇÃO BRASILEIRA DE NORMAS TÉCNICAS, *Materiais pozolânicos – Determinação do índice de desempenho com o cimento Portland aos 28 dias, NBR 5752*, Rio de Janeiro, ABNT, 2014.
- [12] ASSOCIAÇÃO BRASILEIRA DE NORMAS TÉCNICAS, *Cimento Portland e outros materiais em pó – Determinação da massa específica, NBR 16605*, Rio de Janeiro, ABNT, 2017.
- [13] ASSOCIAÇÃO BRASILEIRA DE NORMAS TÉCNICAS, *Agregados – Determinação da massa específica e massa específica aparente, NBR NM 52*, Rio de Janeiro, ABNT, 2009.
- [14] ASSOCIAÇÃO BRASILEIRA DE NORMAS TÉCNICAS, *Agregados – Determinação da massa unitária e volume de vazios, NBR NM 45*, Rio de Janeiro, ABNT, 2006.
- [15] ASSOCIAÇÃO BRASILEIRA DE NORMAS TÉCNICAS, *Agregados para concreto – Especificação, NBR 7211*, Rio de Janeiro, ABNT, 2009. (in portuguese).
- [16] DWIVEDI, V.N., SINGH, N.P., DAS, S.S., *et al.*, “A new pozzolanic material for cement industry: bamboo leaf ash.”, *International Journal of Physical Sciences*, v. 1, n. 3, pp. 106–111, 2006.
- [17] SINGH, N.B., DAS, S.S., SINGH, N.P., *et al.*, “Hydration of bamboo leaf ash blended Portland Cement”, *Indian Journal of Engineering and Materials Sciences*, v. 14, pp. 69–76, 2007.
- [18] VILLAR-COCIÑA, E., MORALES, E.V., SANTOS, S.F., *et al.*, “Pozzolanic behavior of bamboo leaf ash: Characterization and determination of the Kinect parameters”, *Cement and Concrete Composites*, v. 33, n. 1, pp. 68–73, 2010. doi: <http://dx.doi.org/10.1016/j.cemconcomp.2010.09.003>.
- [19] FRÍAS, M., SAVASTANO, H., VILLAR, E., *et al.*, “Characterization and properties of blended cement matrices containing activated bamboo leaf wastes”, *Cement and Concrete Composites*, v. 34, n. 9, pp. 1019–1023, 2012. doi: <http://dx.doi.org/10.1016/j.cemconcomp.2012.05.005>.



- [20] VILLAR-COCIÑA, E., SAVASTANO, H., RODIER, L., *et al.*, “Pozzolanic characterization of cuban bamboo leaf ash: calcining temperature and kinetic parameters”, *Waste and Biomass Valorization*, v. 9, n. 4, pp. 691–699, 2018. doi: <http://dx.doi.org/10.1007/s12649-016-9741-8>.
- [21] RODIER, L., BILBA, K., ONÉSIPPE, C., *et al.*, “Study of pozzolanic activity of bamboo stem ashes for use as partial replacement of cement”, *Materials and Structures*, v. 50, n. 1, pp. 87, 2017. doi: <http://dx.doi.org/10.1617/s11527-016-0958-6>.
- [22] POUHEY, M.T.F., “*Beneficiamento da cinza de casca de arroz residual com vistas à produção de cimento composto e/ou pozolânico*”, D.Sc. Thesis, Universidade Federal do Rio Grande do Sul, Porto Alegre, 2006.
- [23] ASSOCIAÇÃO BRASILEIRA DE NORMAS TÉCNICAS, *Cimento Portland – Determinação da resistência à compressão, NBR 7215*, Rio de Janeiro, ABNT, 1996.
- [24] ASSOCIAÇÃO BRASILEIRA DE NORMAS TÉCNICAS, *Materiais pozolânicos – Requisitos, NBR 12653*, Rio de Janeiro, ABNT, 2014.
- [25] ASSOCIAÇÃO BRASILEIRA DE NORMAS TÉCNICAS, *Cimento Portland composto – Especificação, NBR 11578*, Rio de Janeiro, ABNT, 1991.
- [26] EL-JAZAIRI, B., ILLSTON, J.M.A., “Simultaneous semiisothermal method of thermogravimetry and derivative thermogravimetry, and its application to cement pastes”, *Cement and Concrete Research*, v. 7, n. 3, pp. 247–257, 1977. doi: [http://dx.doi.org/10.1016/0008-8846\(77\)90086-2](http://dx.doi.org/10.1016/0008-8846(77)90086-2).
- [27] MORAES, J.C.B., “*Utilização das cinzas de folha de cana-de-açúcar como material pozolânico em matrizes cimentantes*”, M.Sc. Thesis, Universidade Estadual Paulista, Ilha Solteira. 2015.
- [28] POSSAN, E. “*Contribuição ao estudo da carbonatação do concreto com adição de sílica ativa em ambiente natural e acelerado*”, M.Sc. Thesis, Universidade Federal do Rio Grande do Sul, Porto Alegre, 2004.